Activity-independent and subunit-specific recruitment of functional AMPA receptors at neurexin/neuroligin contacts

Martin Heine[1,2], Olivier Thoumine[1,3], Magali Mondin, Béatrice Tessier, Grégory Giannone, and Daniel Choquet[3]

Centre National de la Recherche Scientifique UMR 5091, Physiologie Cellulaire de la Synapse, Institut François Magendie, Université Bordeaux 2, 33077 Bordeaux, France

A combination of cell culture and animal studies has recently shown that adhesion between neurexins and neuroligins played important roles in synapse initiation, maturation, and function. Binding of neurexin-1β to neuroligin-1 triggers the postsynaptic clustering of the scaffold postsynaptic density protein 95, but the composition and timing of accumulation of glutamate receptors at those nascent contacts remain unclear. Using glutamate iontophoresis and patch-clamp recordings, we identified functional AMPA receptors (AMPARs) and NMDA receptors at postsynaptic density protein 95 clusters induced by neurexin-1β coated microspheres on primary hippocampal neurons. The recruitment of AMPARs occurred as early as 2 h after initial contact, and was not blocked by TTX/2-amino-5-phosphovaleric acid (APV) treatment. The differential recruitment of recombinant subunits GluR1 and GluR2, as well as the absence of rectification in voltage/current curves, further indicate that neurexin/neuroligin contacts primarily recruit GluR2-containing AMPARs. Finally, by using glutamate un-caging and calcium imaging, we show that AMPARs participate in calcium entry at neurexin-1β induced post-synapses, most likely through the activation of voltage-gated calcium channels. Such rapid and activity-independent accumulation of functional AMPARs at neurexin-1β-induced postsynapses points to a new role of AMPARs in synaptogenesis.

glutamate uncaging | glutamate receptors | ionotophoresis | microspheres | postsynaptic density protein 95

The neurexin-neuroligin adhesion complex plays a critical role in brain development and function (1, 2). Neurexins are localized mainly on axons and can form transsynaptic calcium-dependent heterophilic adhesion with neuroligins situated on dendrites (3). Neurexin binds presynaptic adaptors such as Ca^{2+}/calmodulin activated serine-threonine kinase (4), whereas the neuroligin intracellular tail binds the scaffolding postsynaptic density protein 95 (PSD-95) (5, 6). Pathological mutations in neuroligin genes are related to autism and X-linked mental retardation in humans (7–9). In addition, neuroligin-knockout mice die shortly after birth from respiratory failure as a result of reduced network activity in brainstem centers that control respiration (10), and show selectively altered synaptic responses (11). Conversely, studies using α-neurexin-knockout mice demonstrate an essential role of α-neurexins in coupling Ca^{2+} channels to the presynaptic machinery (12) and in maintaining normal postsynaptic NMDA receptor (NMDAR) function (13).

A major role of neurexin-neuroligin adhesion in regulating synaptogenesis has emerged recently from culture studies (14). For example, over-expressing neuroligins in neurons increases synapse density (15), whereas silencing neuroligins induces the opposite (16). Furthermore, primary neurons form functional presynaptic terminals onto HEK cells expressing neuroligin (17–19) and develop postsynaptic scaffolds on fibroblasts expressing neurexin (20). These effects can be mimicked by using microspheres coated with purified neuroligin (21) or neurexin

(20), respectively. However, the kinetics with which newly formed neurexin-induced postsynaptic contacts recruit detectable functional glutamate receptors is unknown. Clusters of neuroligin-1 (Nlg1) and PSD-95 induced by neurexin-1β after a 24 h contact duration positively immunostain for NMDARs, but not for AMPA receptors (AMPARs) (20). Furthermore, the recruitment of AMPARs at neurexin/neuroligin contacts is promoted by glutamate application or constitutively active calmodulin-activated kinase II (CamKII) (22). This differential recruitment of NMDARs and AMPARs is puzzling, as AMPARs could in theory be recruited to the PSD-95 scaffold assembled by neuroligins through binding of their auxiliary subunit stargazin to PSD-95 (23, 24).

An essential question thus remains of whether functional AMPARs are present early on at nascent neurexin-induced postsynaptic differentiations, independently of NMDAR activation, in which case AMPAR activity could play unsuspected roles in regulating synaptogenesis. To address this issue, we induced neuroligin-selective postsynaptic contacts on primary neurons by using neurexin-1β-coated microspheres, independently of preexisting synapses, and characterized their functional properties using local glutamate delivery combined with calcium imaging and electrophysiology.

Results

Neurexin-1β-Coated Beads Induce Nlg1-Selective Postsynaptic Differentiation. To induce selective neurexin-neuroligin contacts, primary rat hippocampal neurons at the onset of synaptogenesis [7–8 days in vitro (DIV)] were incubated with microspheres coated with purified recombinant neurexin1β (Nrx1β-Fc). Nrx1β-Fc beads bound strongly to dendrites and cell bodies, in contrast to control beads coated with Fc alone (Fig. 1*A* and *C*). A treatment with 5 mM EGTA reduced binding by 50% (Fig. 1*C*), suggesting that Nrx1β-Fc ligands interacted in a calcium-dependent manner with endogenous neuroligins on the cell surface (25), but also revealing residual adhesion to unidentified molecules. Furthermore, because Nrx1β can bind equally well to neuroligins 1 and 2, the latter being implicated in inhibitory synapse formation (16, 20, 26), we decided thereafter to transfect Nlg1 to selectively drive the formation of excitatory postsyn-
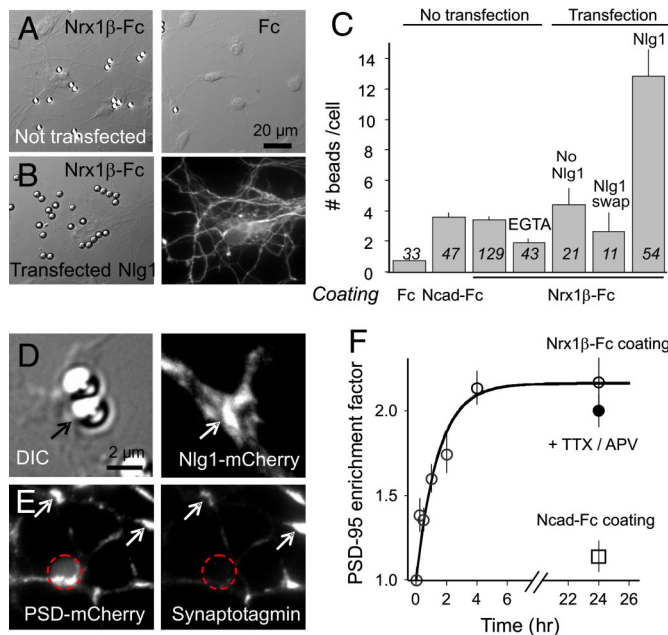
NEUROSCIENCE

Fig. 1. Binding of β-neurexin-coated beads and recruitment of postsynaptic proteins is neuroligin-specific. (*A*) Rat hippocampal neurons at 7 or 8 DIV were incubated with 4-μm microspheres coated with Nrx1β-Fc, N-cadherin-Fc (not shown), or human Fc for 1 h, then rinsed and fixed at given time intervals. Some cultures were co-transfected with PSD-95-GFP and WT Nlg1 (*B*) or an Nlg1 construct unable to interact with neurexin (Nlg1-SWAP). (*C*) Number of beads bound per cell in each condition. Data are presented as mean ± SEM and the number of beads examined is given in italics. (*D*) Example of recruitment of Nlg1-mCherry (arrows) at a Nrx1β-Fc bead. The enrichment factor (bead vs. neurite fluorescence levels) for Nlg1-mCherry was 1.71 ± 0.08 (*n* = 18 beads). (*E*) Example of recruitment of PSD-mCherry; position of the bead is represented by a dashed circle. Immuno-stained synaptotagmin puncta co-localize with spontaneous PSD-95 clusters (arrows), but not with PSD-95-mCherry accumulated at Nrx1β-Fc beads. Neuronal areas covered by synapses were 7.6% ± 1.0% (*n* = 13) outside beads and only 4.5% ± 1.3% (*n* = 48) at Nrx1β-Fc beads, quantitatively showing that Nrx1β-Fc beads do not recruit native synapses. (*F*) Time course of PSD-95-GFP accumulation at Nrx1β-Fc beads, the fit being a first-order exponential function.
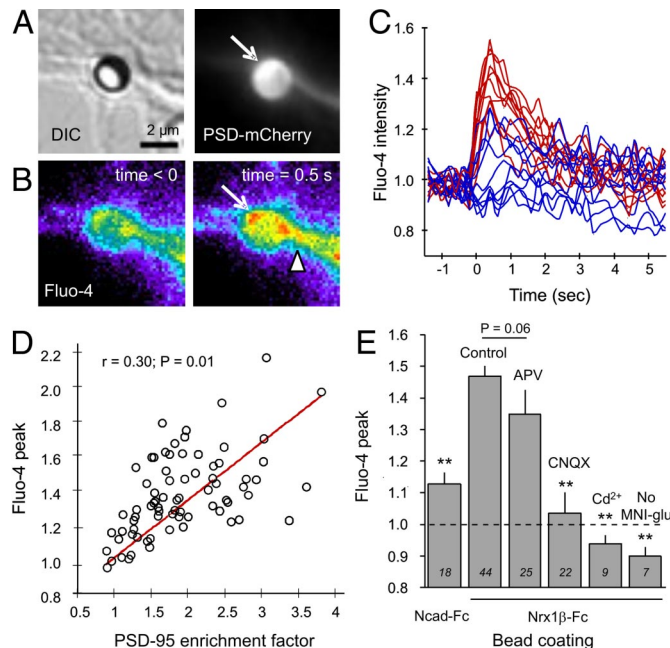
Fig. 2. Glutamate un-caging induces calcium transients at Nrx1β-Fc beads. Neurons co-transfected with Nlg1 and PSD-95-mCherry were incubated overnight with microspheres coated with Nrx1β-Fc. (*A*) Example of a Nrx1β-Fc bead having recruited PSD-95-mCherry. (*B*) Corresponding Fluo-4 signal increase upon photo-release of glutamate at time 0. (*C*) Representative examples of the normalized Fluo-4 fluorescence level over time for 20 beads. Traces in red correspond to beads showing significant PSD-95 recruitment, and those in blue correspond to beads with minimal PSD-95 recruitment. (*D*) Relationship between PSD-95 recruitment level and the peak in Fluo-4 signal elicited upon glutamate un-caging. (*E*) Effect of various treatments on the calcium response, presented as mean ± SEM, where the number of beads tested is indicated in italics. The dashed line represents no change in Fluo-4 level, and responses below this baseline indicate Fluo-4 photo-bleaching. Data were analyzed by one-way ANOVA and compared by Dunnett test to the control Nrx1β-Fc bead condition (**$P < 0.01$).

apses. Neurons transfected with Nlg1 bound three times more Nrx1β-Fc-coated beads than neurons transfected with a neuroligin construct in which the ectodomain was replaced by acetylcholine esterase (Nlg1-SWAP) or non-transfected counterparts (Fig. 1*C*), indicating a functional Nrx1β/Nlg1 interaction. In addition, Nlg1 and PSD-95 accumulated at Nrx1β-Fc beads in large crescent-like patterns (Fig. 1 *D* and *E*), distinct from small endogenous synaptic clusters, which are rather sparse at this developmental stage (27). PSD-95 was recruited by Nrx1β-Fc beads over a time course of 4 h (Fig. 1*F*). Control N-cadherin-Fc coated beads bound as well as Nrx1β-Fc beads (Fig. 1*C*) but did not recruit PSD-95 (Fig. 1*F*), demonstrating the specificity of the assay and confirming the inability of N-cadherin to induce synapse formation (17, 20). Thus, Nrx1β-Fc beads induced neuroligin-specific postsynaptic differentiation.

Calcium Transients Induced by Glutamate Un-Caging at Nrx1β-Fc Beads. To test for the presence of functional glutamate receptors at Nrx1β-Fc microsphere contacts, we first used a global approach based on glutamate photo-release and calcium imaging. Cells were transfected with PSD-mCherry as a live marker of postsynaptic differentiation, and loaded with the fluorescent calcium indicator Fluo-4. The observation medium contained 4-methoxy-7-nitroindolinyl-caged l-glutamate, which caused no apparent excitotoxicity (28, 29), together with glycine and no

magnesium to favor the opening of NMDAR channels. Upon un-caging of glutamate in the vicinity of microspheres, we recorded significant Fluo-4 fluorescence increase at microspheres that had recruited PSD-mCherry (Fig. 2*A* and *B*). Calcium signals originated from the bead contact, sometimes precisely at locations showing PSD-95 accumulation, then rapidly diffused into the dendrite (Fig. 2*B*). There was no such increase when 4-methoxy-7-nitroindolinyl-caged l-glutamate was omitted from the extracellular medium (Fig. 2*E*), indicating a specific response to glutamate release and not photo-damage. On average, the Fluo-4 level increased by 45% in 0.5 sec, then decreased to baseline level with a characteristic decay time of 2 sec (Fig. 2 *C* and *E*). In contrast, beads showing weak or no PSD-mCherry recruitment induced only small calcium transients (Fig. 2 *C* and *D*). Overall, the glutamate-induced calcium increase correlated well with the level of PSD-95 enrichment at bead contacts (Fig. 2*D*), suggesting that functional glutamate receptors were recruited via PSD-95 molecules clustered at neurexin/neuroligin contacts. Control beads coated with N-cadherin-Fc, or neurite areas without beads, elicited only minor calcium responses (Fig. 2*E*), probably because of the presence of sparse endogenous synapses.

To identify which glutamate receptor subtypes were recruited at Nrx1β-induced contacts, we used a pharmacological approach. Surprisingly, treatment with the NMDAR antagonist 2-amino-5-phosphovaleric acid (APV) caused only a 20% reduction in the calcium response (Fig. 2*E*). This indicated that NMDARs were

present at Nrx1β-Fc microsphere contacts, but were not the main mediator of calcium entry. In contrast, treatment with the AMPAR antagonist CNQX (6-cyano-7-nitroquinoxaline-2,3-dione) inhibited the calcium response by 90% (Fig. 2E), suggesting the presence of functional AMPARs at Nrx1β-Fc beads. The majority of AMPARs in hippocampal neurons contain the GluR2-subunit, which is weakly permeable to calcium (30). Thus, we hypothesized that AMPARs caused membrane depolarization which, in turn, led to activation of voltage-gated calcium channels located nearby in the dendrite (31). Indeed, treatment with cadmium, a broad-spectrum blocker of calcium-permeable channels including NMDARs (32), completely abolished Fluo-4 transients (Fig. 2E).

Patch-Clamp Currents Evoked by Iontophoretic Glutamate Application at Nrx1β-Fc Beads Reveal Functional AMPARs and NMDARs. To directly identify the presence of functional NMDARs and AMPARs at neurexin/neuroligin contacts and characterize their kinetics of recruitment compared with native synapses, we performed whole-cell patch-clamp recordings together with local glutamate application at Nrx1β-Fc beads by using iontophoresis (Fig. 3A). Cells were transfected with PSD-95-GFP to visualize postsynaptic differentiation (Fig. 3B). Beads displaying PSD-95-GFP accumulation usually exhibited the strongest currents (Fig. 3C). On average, Nrx1β-Fc beads incubated for 24 h had current amplitudes of 256 ± 40 pA (n = 25 beads), more than twofold that of endogenous PSD-95 clusters (120 ± 18 pA, n = 22) or beads incubated for only 2 to 4 h (105 ± 24 pA, n = 11). Control neurite regions with homogeneous PSD-95 distribution, as well as N-cadherin-Fc-coated beads, produced much smaller currents, i.e., 19 ± 7 pA (n = 6) and 13 ± 4 pA (n = 13), respectively. The increase in current amplitude from 2–4 h to 24 h paralleled the time course of PSD-95 accumulation (Fig. 1F), further indicating that the presence of PSD-95 and functional glutamate receptors were associated.

The shape of the currents at Nrx1β-Fc beads indicated both a fast AMPAR component and a slow NMDAR component. Indeed, the slow phase disappeared in the presence of the NMDAR antagonist APV, and the remaining fast response was blocked by the AMPAR antagonist CNQX (Fig. 3D). The fact that the AMPAR and NMDAR components could easily be distinguished on a time scale basis allowed the systematic computation of the relative AMPAR charge by using bi-exponential fitting of the current/time curves obtained in the absence of pharmacological treatment. AMPARs mediated 18% of the total charge transfer 2 to 4 h after initial bead contact, and after 24 h this proportion reached 30% (Fig. 3F), approximately that of established synapses (Fig. 3E). It is unlikely that the progressive increase of AMPAR charge at Nrx1β-Fc beads can be explained by a parallel replacement of NR1/NR2B by NR1/NR2A heteromers with faster desensitization kinetics, which could lead to an overestimation of the AMPAR component. Indeed, the switch in NMDAR subunit composition linked to synapse maturation occurs on a longer time course, typically from 6 to 15 DIV (33). Furthermore, the slower rate constant representing NMDARs did not differ significantly between the 2–4 h and 24 h time points, i.e., 166 ± 32 ms (n = 8) versus 197 ± 29 ms (n = 12), respectively.

As it was previously suggested that the synapse promoting effect of Ngl1 was dependent on NMDAR activity (22), we treated neurons with TTX to suppress action potential driven network activity and APV to block NMDAR function during the 24-h bead contact. In these conditions, the recruitment of PSD-95 (Fig. 1F) as well as the fast AMPAR current component were still present (Fig. 3F), demonstrating that the accumulation of functional postsynaptic AMPARs does not require sustained neuronal activity. TTX/APV treatment instead caused an increase in AMPAR charge both at Nrx1β beads (Fig. 3F) and synapses labeled by PSD-95 clusters (Fig. 3E), as well as a
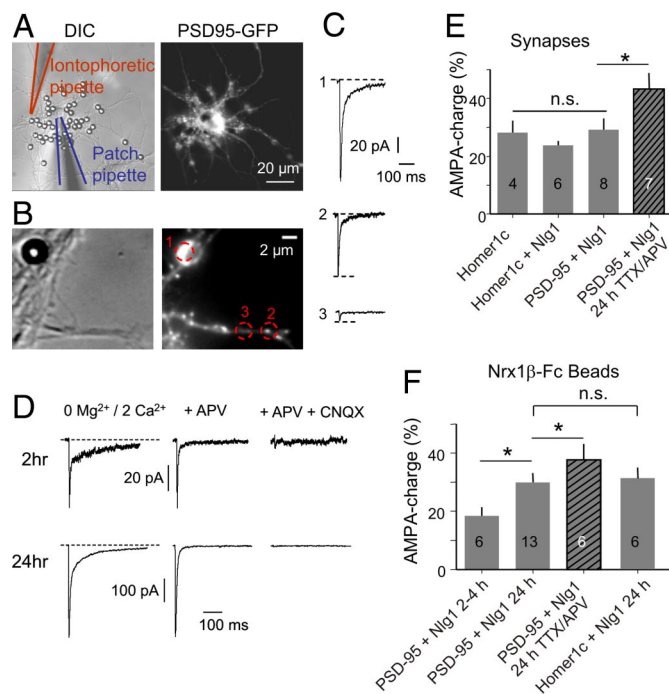

Fig. 3. Characterization of glutamate receptor composition at Nrx1β-Fc beads by glutamate ionotophoresis and patch-clamp experiment. Neurons co-transfected with Nlg1 and PSD-95-GFP (or Homer1c-GFP) were left in contact with Nrx1β-Fc-coated microspheres for 2–4 h or 24 h, then subjected to whole-cell electrophysiology in the presence of TTX to prevent action potentials and 0 mM Mg to remove the NMDAR block. In some experiments, cells were treated with TTX and APV throughout the bead incubation (24 h). (A) Digital image correlation showing patch-clamp and iontophoresis pipettes, with the corresponding PSD-95-GFP fluorescence. Note that many beads bind to the transfected cell. (B) Magnified view of accumulation of PSD-95-GFP surrounding a Nrx1β-Fc bead and nearby synaptic clusters. (C) Examples of currents elicited upon glutamate application at Nrx1β-Fc beads (trace 1), endogenous PSD-95-GFP clusters (trace 2), or neurite region without PSD-95 accumulation (trace 3), with the membrane potential being clamped at −60 mV. (D) Effect of NMDAR and AMPAR antagonists (CNQX and APV, respectively) on the electrophysiological response of βNrx1β-Fc bead contacts at two contact durations. (E and F) By fitting the curves using a bi-exponential function with two separate time constants, the relative charge carried by AMPARs was computed for various conditions. (E) Synapses identified by PSD-95-GFP or Homer1c-GFP positive puncta. (F) Nrx1β-Fc beads displaying recruitment of PSD-95-GFP or Homer1c-GFP. Data were analyzed by one-way ANOVA and compared two-by-two by Tukey test (*, P < 0.05; ns, not significant).

stronger immunostaining of endogenous AMPAR at PSD-95 clusters [supporting information (SI) Fig. S1]. These events are most likely linked to an homeostatic increase in AMPAR surface expression (34, 35).

As PSD-95 over-expression is known to drive GluR1 to nascent synapses and increase AMPAR synaptic currents (23, 36), whereas PSD-95 KO decreases AMPAR synaptic transmission by increasing the number of silent synapses (37), we performed control experiments using Homer1c, a non-perturbing postsynaptic marker (38). The AMPAR charge measured at synaptic clusters did not differ significantly between neurons co-transfected with Nlg1 and either PSD-95-GFP or Homer1c-GFP (Fig. 3E). Moreover, Homer1c was recruited to Nrx1β-Fc beads, albeit to a lesser degree than PSD-95, and those beads still exhibited significant AMPAR currents (Fig. 3F). This shows that, in our conditions, AMPARs can be recruited at Nrx1β-induced contacts under endogenous PSD-95 levels. AMPAR recruitment was also not an artifact of Nlg1 over-expression, as Nlg1 transfection per se does not increase
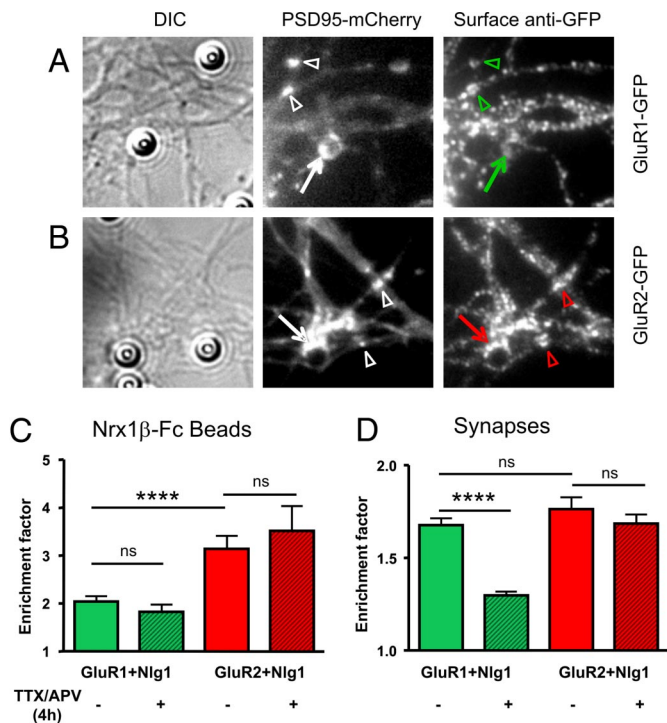
Fig. 4. Recruitment of recombinant AMPAR subunits at Nrx1β-Fc beads and synapses. Neurons were transfected with Nlg1 and PSD-95-mCherry plus either GluR1-GFP or GluR2-GFP, incubated for 4 h with Nrx1β-Fc beads with or without TTX/APV, then processed for live anti-GFP staining. Examples of recombinant GluR1 (*A*) or GluR2 (*B*) stainings at Nrx1β-Fc beads (arrows) and nearby endogenous synapses, as identified by PSD-95-mCherry clusters (arrowheads). Quantification of the enrichment factor, i.e., the fluorescence signal on a bead (*C*) or synapse (*D*) divided by the neurite level, for all conditions. The number of beads or clusters quantified is given in each column. Data were analyzed by one-way ANOVA and compared by Tukey test (***, *P* < 0.0002).

AMPAR receptor abundance at synapses, as assessed from the amplitude of miniature AMPA currents (15). Accordingly, we found that the AMPAR charge at synapses labeled with Homer 1c-GFP was not changed upon additional expression of Nlg1 (Fig. 3*E*). The absence of rectification at positive membrane potentials in the current/voltage curves indicates that AMPARs present at Nrx1β-Fc beads were mostly composed of GluR2-containing heteromers (Fig. S2). Finally, we performed live AMPAR surface staining and detected strong labeling at Nrx1β-Fc beads, but not at N-cadherin-Fc-coated beads (Fig. S3), confirming the specific presence of AMPARs at Nrx1β/Nlg1 contacts by immunohistochemistry.

Differential Recruitment of GluR1 and GluR2 AMPAR Subunits at Nrx1β-Fc Beads. To examine in more detail the subunit specificity of AMPAR recruitment at Nrx1β/Nlg1 contacts, we co-transfected neurons with Nlg1 together with recombinant GFP-tagged GluR1 or GluR2 subunits. The recruitment of membrane-associated AMPARs at Nrx1β-Fc beads bound for 4 h was detected by live surface staining with anti-GFP antibodies (Fig. 4 *A* and *B*). In half the experiments, PSD-mCherry was co-transfected, whereas in the other half, endogenous PSD-95 was immunostained. The enrichment level of endogenous PSD-95 (2.6 ± 0.1, *n* = 106) was similar to that of PSD-mCherry (2.6 ± 0.2, *n* = 68), and there was little effect of exogenous PSD-mCherry expression on the recruitment of either GluR1 or GluR2 (not shown), so we pooled the data from both conditions (Fig. 4). The striking result was that GluR2 was strongly recruited at Nrx1β-Fc beads (Fig. 4 *B* and *C*), whereas GluR1 was
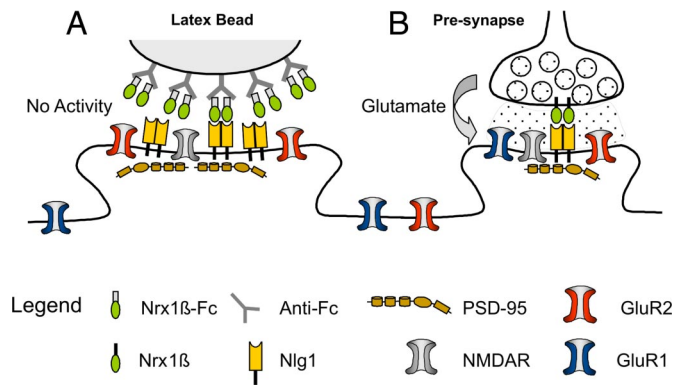

Fig. 5. Comparison of postsynapses triggered by Nrx1β to endogenous synapses. (*A*) Nrx1β-Fc beads not exposed to chronic glutamate release induce the clustering of PSD-95, NMDAR, and GluR2-containing AMPAR, but exclude GluR2-lacking AMPAR receptors. (*B*) In contrast, synapses recruit GluR1-containing AMPAR in an activity-dependent manner.

almost absent (Fig. 4 *A* and *C*). The recruitment levels were not affected by a 4-h treatment with APV/TTX during bead incubation (Fig. 4*C*). By comparison, GluR1 and GluR2 were enriched to similar levels at endogenous synapses identified by PSD-mCherry fluorescence (Fig. 4 *A*, *B* and *D*). The TTX/APV treatment reduced the synaptic GluR1 level, leaving GluR2 staining intact (Fig. 4*D*). Thus, GluR1 is recruited at synaptic contacts in an activity-dependent manner, and absent from Nrx1β-induced postsynapses, which are not linked to presynaptic activity; whereas GluR2 is recruited both at Nrx1β/Nlg1 contacts and nascent synapses in a rather constitutive fashion (Fig. 5).

Discussion

Both NMDA and AMPA Receptors Are Recruited at Neurexin/Neuroligin Contacts. We showed here, by using a minimal constituent system, that mobilizing Nlg1 molecules by Nrx1β binding drives functional postsynapse assembly, characterized by calcium responses and the rapid recruitment of NMDARs and AMPARs, closely following the appearance of PSD-95. Note that this is basically the reverse of previous experiments that used HEK cells co-transfected with Nlg1 and NMDAR (18) or AMPAR (19) subunits. There, the patch-clamp currents recorded in HEK cells revealed the presence of glutamate release at presynaptic terminals formed by axons of co-cultured neurons onto the heterologous cells. Conversely, we demonstrate here the spontaneous assembly of functional glutamate receptors at Nrx1β-induced postsynapses in dendrites, in the absence of presynapses. Advantages of the microsphere assay are that we could isolate selective effects of the neurexin/neuroligin interaction independently of other synaptogenic proteins such as SynCAM (19), and precisely control the initial encounter time. One drawback was that we had to transfect Nlg1 to ensure a specific Nrx1β/Nlg1 interaction, given the limited effects of Nrx1β-Fc beads on un-transfected cells. This may originate from the bead coating protocol, which yielded a fairly low density of immobile Nrx1β ligands (approximately 500 dimers/μm^2) (39). As a result, the local number of endogenous interacting proteins might be too small to trigger postsynapse differentiation, in contrast with native synapses in which Nrx1β/Nlg1 bonds might reach higher concentrations because molecules can slide laterally in the plasma membrane and cluster more efficiently. For example, presynaptic differentiation was obtained only with lipid-coated microspheres bearing freely diffusing GPI-anchored Nlg1 (21). Nevertheless, as pointed out earlier, Nlg1 over-expression does not seem to affect the postsynaptic targeting of AMPARs.

In those conditions, PSD-95 could be detected by 1 h after adhesive contact and reached a maximum level by 4 h. The AMPA/NMDA current fraction increased progressively over time (from 2 h to 24 h), suggesting that AMPARs appear slightly later than NMDARs. The time course obtained here with selective Nrx1β-triggered adhesions agrees with that reported for spontaneous axo-dendritic contacts (40), suggesting that during the formation of native synapses, neurexin/neuroligin binding plays a key role in the recruitment of specific postsynaptic components. Immunostaining using antibodies against an intracellular epitope of NR1 had previously indicated the presence of NMDARs at contacts between neurons and fibroblasts expressing β-neurexin (20). Our results now establish that NMDARs are present in the neuronal plasma membrane and functional at neurexin/neuroligin contacts. Such recruitment of NMDARs may involve a pivotal role of PSD-95, which can bind concomitantly the Nlg1 intracellular tail (41) and NMDAR subunits (42).

Selective Recruitment of GluR2-Containing AMPARs. The identification of AMPARs at Nrx1β-Fc beads was more surprising because they were not previously detected by immunocytochemistry in the co-culture assay under resting conditions (20). Although the experimental conditions are very close, this discrepancy may originate from difficulties to immunostain AMPAR. Indeed, we were unable to label GluR2 with commercial antibodies, and obtained a specific signal only by live staining with a highly specific anti-GluR1 antibody, likely to stain endogenous GluR1/GluR2 heteromers. We thus believe the functional assays described here are more sensitive than immuno-cytochemistry. In another study, GluR1-containing AMPARs were detected at neuronal contacts with PC12 cells expressing Nrx1β only upon stimulation with glutamate or a constitutively active CamKII mutant (22). Here, confirming this previous result, we showed that over-expressed GluR1 subunits, likely to form calcium-permeable GluR1 homomers (43), are indeed not recruited at Nrx1β-Fc beads, whereas GluR2 subunits strongly accumulate. The comparison with preexisting synapses is striking, as GluR1 and GluR2 subunits are found equally present in control conditions. The synaptic enrichment of the GluR1 subunit was reduced by a 4-h TTX/APV treatment, confirming that the accumulation of GluR1-containing AMPARs at postsynapses requires synaptic activity. Because there is no glutamatergic release in front of Nrx1β-Fc beads, GluR1-containing AMPARs are naturally excluded from them. In that sense, Nrx1β-induced postsynapses resemble synapses in which the presynaptic release machinery has been chronically silenced, as these are unable to trap postsynaptic GluR1-containing AMPARs (44). In contrast, GluR2-containing AMPARs accumulate in a constitutive fashion at Nrx1β-Fc beads and are not sensitive to activity blockade at preexisting synapses. The preferential presence of GluR2-containing receptors at neurexin/neuroligin contacts is sustained by two additional observations: (*i*) the current/voltage curves obtained by patch-clamp experiments upon glutamate iontophoresis at Nrx1β-Fc beads showed no rectification; and (*ii*) cadmium, which does not affect the calcium permeability of GluR2-lacking AMPARs (45), efficiently blocked calcium entry at Nrx1β-Fc beads induced by glutamate un-caging. These findings agree with the fact that the expression of Nlg1 lacking its C terminus—and thus unable to interact with PSD-95—reduces both the amplitude of AMPA miniature excitatory postsynaptic currents and GluR2 labeling at native synapses (22).

Activity-Independent Recruitment of AMPARs at Neurexin/Neuroligin Contacts. Although there are very few synapses in such young cultures and no accumulation of functional presynaptic terminals at bead contacts, it was still possible that endogenous AMPAR

recruitment was triggered by the stimulation of NMDARs initially present at Nrx1β-Fc beads through glutamate spill-over from neighboring synapses. To rule out this possibility, we treated the cultures with the activity blockers TTX and APV for 24 h, which did not affect the accumulation of PSD-95 at Nrx1β-Fc beads. Far from inhibiting AMPAR recruitment, we instead found a significant increase of AMPAR charge detected at Nrx1β-Fc beads and synapses, as well as an increase in AMPAR staining at PSD-95 puncta. These findings agree with a previous report showing that TTX/APV treatment, by blocking NMDAR miniature excitatory postsynaptic currents, potentiates the effect of TTX alone (35) and induces a strong homeostatic up-scaling of AMPAR availability by triggering local protein translation and membrane delivery (34). This effect is contrary to the more classical increase in GluR1-containing AMPARs at mature synapses triggered by plasticity protocols (43), and seems to be specific to immature synapses (46). The fact that scaling was more pronounced for endogenous synapses than for beads also calls for a local regulation. At shorter term (4 h), we found no effect of TTX/APV on the recruitment of recombinant GluR1 or GluR2 AMPAR subunits at Nrx1β-Fc beads. Such lack of effect of NMDAR blockade on AMPAR recruitment at neurexin/neuroligin adhesions apparently contrasts with a recent study that showed that the synaptogenic effect of Nlg1 is reversed by chronic treatment with NMDAR or CamKII inhibitors (11). These authors propose that the increase in synapse density taking place upon Nlg1 over-expression is not the result of initial adhesion between dendritic Nlg1 and axonal Nrx1β (21), but of a more complex regulation of Nlg1 function by NMDAR activation implicated in the later stages of synapse maturation (11). The mechanism is unclear at present, but could involve a retrograde signaling that influences presynaptic assembly and glutamate release (47). However, it is also possible that, during such a long-term APV treatment (4 d) that caused chronic reduction of postsynaptic calcium entry, other molecular pathways might develop independently of Nlg1. We thus believe that this mechanism of long-term presynapse assembly is different from the rapid postsynaptic differentiation described here, which by no means involves active presynapses.

Mechanisms and Functional Role of AMPAR Mobilization at Neurexin/Neuroligin Contacts. The fact that the presence of AMPARs at neurexin/neuroligin contacts was closely associated with the level of PSD-95 suggests a close relationship between the two molecules. As AMPARs do not bind PSD-95 directly, it is tempting to speculate that membrane AMPARs associate with PSD-95 clusters triggered by neurexin/neuroligin interaction through the auxiliary subunit stargazin (48), which binds PDZ domains 1 and 2 of PSD-95 (23) and stabilize surface-diffusing AMPARs at synapses (24). Such a trapping mechanism would suggest a relevant function for relatively abundant extrasynaptic AMPARs in young neurons (27), the role of which remain elusive. Alternative models such as regulated insertion and removal of AMPARs from the cell surface may also be implicated (49). We are currently developing a high-throughput assay to trigger the rapid formation of hemi postsynapses, which will allow us to screen biological conditions to discriminate between the possible mechanisms of glutamate receptor recruitment. In any case, the presence of functional AMPARs at nascent neuronal contacts initiated by neurexin-neuroligin binding suggests that they may play an unsuspected role in activity-dependent regulation of synapse formation. For example, we showed that AMPARs participate in calcium signaling at β-neurexin-induced postsynapses, most likely through the activation of voltage-gated calcium channels (31). Also, chronic AMPAR blockade suggests an important impact of functional AMPARs in maintaining synaptic structure and function (50). The activation of AMPARs by miniature glutamate release at newly formed synapses (34)

NEUROSCIENCE

may contribute to the stabilization and plastic properties of these contacts, and therefore play a crucial role right at the beginning of the establishment of a new synapse.

Methods

Briefly, primary rat hippocampal neurons were transfected at 4 or 5 DIV with various combinations of the following plasmids: Nlg1-HA, Nlg1-mCherry, PSD-95-GFP, PSD-95 mCherry, Homer1c-GFP, GluR1-GFP, and GluR2-GFP. Neurons at 7 or 8 DIV were incubated with microspheres coated with Nrx1β-Fc or N-cadherin-Fc as a control, for times ranging from 2 h to 24 h. Three types of experiments were carried out: (*i*) immuno-cytochemistry to detect enrichment levels of Nlg1, PSD-95, or GluRs at bead contacts or synapses; (*ii*) glutamate un-caging and calcium imaging using a bi-photon confocal microscope; and (*iii*) glutamate iontophoresis and patch-clamp recordings. All protocols are described thoroughly in *SI Methods*.

1. Missler M, Sudhof TC (1998) Neurexins: three genes and 1001 products. *Trends Genet* 14:20–26.
2. Craig AM, Kang Y (2007) Neurexin-neuroligin signaling in synapse development. *Curr Opin Neurobiol* 17:43–52.
3. Levinson JN, El-Husseini A (2007) A crystal-clear interaction: relating neuroligin/neurexin complex structure to function at the synapse. *Neuron* 56:937–939.
4. Missler M, Fernandez-Chacon R, Sudhof TC (1998) The making of neurexins. *J Neurochem* 71:1339–1347.
5. Ichtchenko K, *et al.* (1995) Neuroligin 1: a splice site-specific ligand for beta-neurexins. *Cell* 81:435–443.
6. Irie M, *et al.* (1997) Binding of neuroligins to PSD-95. *Science* 277:1511–1515.
7. Jamain S, *et al.* (2003) Mutations of the X-linked genes encoding neuroligins NLGN3 and NLGN4 are associated with autism. *Nat Genet* 34:27–29.
8. Laumonnier F, *et al.* (2004) X-linked mental retardation and autism are associated with a mutation in the NLGN4 gene, a member of the neuroligin family. *Am J Hum Genet* 74:552–557.
9. Tabuchi K, *et al.* (2007) A neuroligin-3 mutation implicated in autism increases inhibitory synaptic transmission in mice. *Science* 318:71–76.
10. Varoqueaux F, *et al.* (2006) Neuroligins determine synapse maturation and function. *Neuron* 51:741–754.
11. Chubykin AA, *et al.* (2007) Activity-dependent validation of excitatory versus inhibitory synapses by neuroligin-1 versus neuroligin-2. *Neuron* 54:919–931.
12. Missler M, *et al.* (2003) Alpha-neurexins couple Ca2+ channels to synaptic vesicle exocytosis. *Nature* 423:939–948.
13. Kattenstroth G, *et al.* (2004) Postsynaptic N-methyl-D-aspartate receptor function requires alpha-neurexins. *Proc Natl Acad Sci USA* 101:2607–2612.
14. Craig AM, Graf ER, Linhoff MW (2006) How to build a central synapse: clues from cell culture. *Trends Neurosci* 29:8–20.
15. Levinson JN, *et al.* (2005) Neuroligins mediate excitatory and inhibitory synapse formation: involvement of PSD-95 and neurexin-1beta in neuroligin-induced synaptic specificity. *J Biol Chem* 280:17312–17319.
16. Chih B, Engelman H, Scheiffele P (2005) Control of excitatory and inhibitory synapse formation by neuroligins. *Science* 307:1324–1328.
17. Scheiffele P, *et al.* (2000) Neuroligin expressed in nonneuronal cells triggers presynaptic development in contacting axons. *Cell* 101:657–669.
18. Fu Z, Washbourne P, Ortinski P, Vicini S (2003) Functional excitatory synapses in HEK293 cells expressing neuroligin and glutamate receptors. *J Neurophysiol* 90:3950–3957.
19. Sara Y, *et al.* (2005) Selective capability of SynCAM and neuroligin for functional synapse assembly. *J Neurosci* 25:260–270.
20. Graf ER, *et al.* (2004) Neurexins induce differentiation of GABA and glutamate postsynaptic specializations via neuroligins. *Cell* 119:1013–1026.
21. Dean C, *et al.* (2003) Neurexin mediates the assembly of presynaptic terminals. *Nat Neurosci* 6:708–716.
22. Nam CI, Chen L (2005) Postsynaptic assembly induced by neurexin-neuroligin interaction and neurotransmitter. *Proc Natl Acad Sci USA* 102:6137–6142.
23. Schnell E, *et al.* (2002) Direct interactions between PSD-95 and stargazin control synaptic AMPA receptor number. *Proc Natl Acad Sci USA* 99:13902–13907.
24. Bats C, Groc L, Choquet D (2007) The interaction between stargazin and PSD-95 regulates AMPA receptor surface trafficking. *Neuron* 53:719–734.
25. Comoletti D, *et al.* (2003) Characterization of the interaction of a recombinant soluble neuroligin-1 with neurexin-1beta. *J Biol Chem* 278:50497–50505.
26. Varoqueaux F, Jamain S, Brose N (2004) Neuroligin 2 is exclusively localized to inhibitory synapses. *Eur J Cell Biol* 83:449–456.
27. Cottrell JR, Dube GR, Egles C, Liu G (2000) Distribution, density, and clustering of functional glutamate receptors before and after synaptogenesis in hippocampal neurons. *J Neurophysiol* 84:1573–1587.
28. Matsuzaki M, *et al.* (2001) Dendritic spine geometry is critical for AMPA receptor expression in hippocampal CA1 pyramidal neurons. *Nat Neurosci* 4:1086–1092.
29. Sobczyk A, Scheuss V, Svoboda K (2005) NMDA receptor subunit-dependent [Ca2+] signaling in individual hippocampal dendritic spines. *J Neurosci* 25:6037–6046.
30. Cull-Candy S, Kelly L, Farrant M (2006) Regulation of Ca2+-permeable AMPA receptors: synaptic plasticity and beyond. *Curr Opin Neurobiol* 16:288–297.
31. Magee JC, Johnston D (1995) Synaptic activation of voltage-gated channels in the dendrites of hippocampal pyramidal neurons. *Science* 268:301–304.
32. Mayer ML, Vyklicky L, Jr., Westbrook GL (1989) Modulation of excitatory amino acid receptors by group IIB metal cations in cultured mouse hippocampal neurones. *J Physiol* 415:329–350.
33. Groc L, *et al.* (2006) NMDA receptor surface mobility depends on NR2A–2B subunits. *Proc Natl Acad Sci USA* 103:18769–18774.
34. Sutton MA, *et al.* (2006) Miniature neurotransmission stabilizes synaptic function via tonic suppression of local dendritic protein synthesis. *Cell* 125:785–799.
35. Watt AJ, *et al.* (2000) Activity coregulates quantal AMPA and NMDA currents at neocortical synapses. *Neuron* 26:659–670.
36. El-Husseini AE, *et al.* (2000) PSD-95 involvement in maturation of excitatory synapses. *Science* 290:1364–1368.
37. Beique JC, *et al.* (2006) Synapse-specific regulation of AMPA receptor function by PSD-95. *Proc Natl Acad Sci USA* 103:19535–19540.
38. Usui S, *et al.* (2003) Synaptic targeting of PSD-Zip45 (Homer 1c) and its involvement in the synaptic accumulation of F-actin. *J Biol Chem* 278:10619–10628.
39. Thoumine O, Lambert M, Mege RM, Choquet D (2006) Regulation of N-cadherin dynamics at neuronal contacts by ligand binding and cytoskeletal coupling. *Mol Biol Cell* 17:862–875.
40. Friedman HV, Bresler T, Garner CC, Ziv NE (2000) Assembly of new individual excitatory synapses: time course and temporal order of synaptic molecule recruitment. *Neuron* 27:57–69.
41. Song JY, Ichtchenko K, Sudhof TC, Brose N (1999) Neuroligin 1 is a postsynaptic cell-adhesion molecule of excitatory synapses. *Proc Natl Acad Sci USA* 96:1100–1105.
42. Niethammer M, Kim E, Sheng M (1996) Interaction between the C terminus of NMDA receptor subunits and multiple members of the PSD-95 family of membrane-associated guanylate kinases. *J Neurosci* 16:2157–2163.
43. Shi S, Hayashi Y, Esteban JA, Malinow R (2001) Subunit-specific rules governing AMPA receptor trafficking to synapses in hippocampal pyramidal neurons. *Cell* 105:331–343.
44. Ehlers MD, *et al.* (2007) Diffusional trapping of GluR1 AMPA receptors by input-specific synaptic activity. *Neuron* 54:447–460.
45. Fischer W, *et al.* (2002) AMPA-induced Ca(2+) influx in cultured rat cortical nonpyramidal neurones: pharmacological characterization using fura-2 microfluorimetry. *Eur J Pharmacol* 438:53–62.
46. Hall BJ, Ghosh A (2008) Regulation of AMPA receptor recruitment at developing synapses. *Trends Neurosci* 31:82–89.
47. Futai K, *et al.* (2007) Retrograde modulation of presynaptic release probability through signaling mediated by PSD-95-neuroligin. *Nat Neurosci* 10:186–195.
48. Chen L, *et al.* (2000) Stargazin regulates synaptic targeting of AMPA receptors by two distinct mechanisms. *Nature* 408:936–943.
49. Barry MF, Ziff EB (2002) Receptor trafficking and the plasticity of excitatory synapses. *Curr Opin Neurobiol* 12:279–286.
50. Mateos JM, *et al.* (2007) Synaptic modifications at the CA3-CA1 synapse after chronic AMPA receptor blockade in rat hippocampal slices. *J Physiol* 581:129–138.